Structures of AlN/VN superlattices with different AlN layer thicknesses

Quan Li[a)]
Department of Physics, The Chinese University of Hong Kong, Shatin, New Territory, Hong Kong
I.W. Kim, S.A. Barnett, and L.D. Marks
Department of Material Science & Engineering, Northwestern University, Evanston, Illinois 60208

(Received 16 December 2001; accepted 5 March 2002)

AlN/VN superlattices with different periods were studied using x-ray diffraction and transmission electron microscopy (TEM). A phase transformation of the AlN from an epitaxially stabilized rock-salt structure to a hexagonal wurtzite structure was observed for an AlN layer thickness greater than 4 nm. A structural model is proposed on the basis of TEM results for the orientation of the transformed phase. The VN layer grown on top of the hexagonal AlN was observed to be reoriented compared to that in the stabilized B1-AlN/VN. The VN nucleated by taking the w-AlN(002) plane as its (111) plane instead of the (002) plane.

I. INTRODUCTION

AlN, one of the III–V compounds, is characterized by high ionicity, short bond length, low compressibility, high thermal conductivity, and a wide band gap. These properties make it interesting and useful in many areas, for instance applications for lasers and high-temperature transistors. At ambient temperature and pressure, AlN has a wurtzite (w-AlN) structure with alternating layers of Al and N atoms. A high-pressure rock-salt (B1-AlN) structure and a zinc-blende (zb-AlN) structure were predicted by Christensen *et al.* using total energy calculations.[1,2] Both of them are cubic structures, as shown in Fig. 1. A pressure-induced first-order transition from the hexagonal to the B1 structure has been observed in bulk AlN, in reasonable agreement with theory.[3,4]

An alternative method of obtaining the metastable cubic phase is epitaxial stabilization. In a previous study, zinc-blende AlN was observed to be stabilized in an AlN/W superlattice, in which zb-AlN transformed to w-AlN at larger thickness;[5] B1-AlN was observed to be stabilized in both AlN/NbN[6] and AlN/TiN[7] superlattices with an AlN layer thickness of less than 2.0 nm. More recently it was found that B1-AlN could also be stabilized in AlN/VN (001) superlattices with an AlN layer thickness of less than 4.0 nm, the largest critical thickness obtained to date.[8] This is due to the smaller lattice mismatch between B1-AlN and VN. Relatively little is known about the B1 to hexagonal transformation.

In this paper, we report results showing the epitaxial stabilization of B1-AlN in AlN/VN superlattices with an AlN layer thickness less than 4.0 nm. A phase transformation from B1-AlN to w-AlN takes place when the AlN layer thickness exceeds the 4.0-nm critical thickness. Cross-sectional high-resolution electron microscopy (HREM) observations of the superlattice layers also show a reorientation of the VN layer above the w-AlN layer. Both the orientation of the transformed w-AlN as well as that of the subsequent VN can be understood as minimizing the misfit stresses. The relative orientation of the transformed w-AlN, as well as observation of a very small fraction of retained B1-AlN, suggests that the phase transition is martensitic.

II. EXPERIMENTAL PROCEDURES

AlN/VN superlattices were grown on MgO(001) substrates in an ultrahigh vacuum dc-magnetron sputtering system that has been described elsewhere.[9] The sputtering targets were 99.95% pure V and 99.99% pure Al. Superlattices were deposited in mixtures of 12 mtorr of Ar and 3.6 mtorr of N_2. The MgO(001) substrates were first cleaned in organic solvents and then annealed at 750 °C in vacuum for 0.5 h. After that, the substrate temperature was dropped to 630 °C, which proved (from experiments at different temperatures) to be the optimal operating temperature. All buffer layers and superlattices were deposited at this temperature. In all cases, a 200-nm VN buffer layer was deposited prior to superlattice deposition. With a constant VN layer thickness of 2.5 nm, two samples (nos. 1 and 2) with different AlN layer thickness (1.3 and 5.0 nm, respectively) were deposited for x-ray

[a)]Address all correspondence to this author.
e-mail: liquan@phy.cuhk.edu.hk

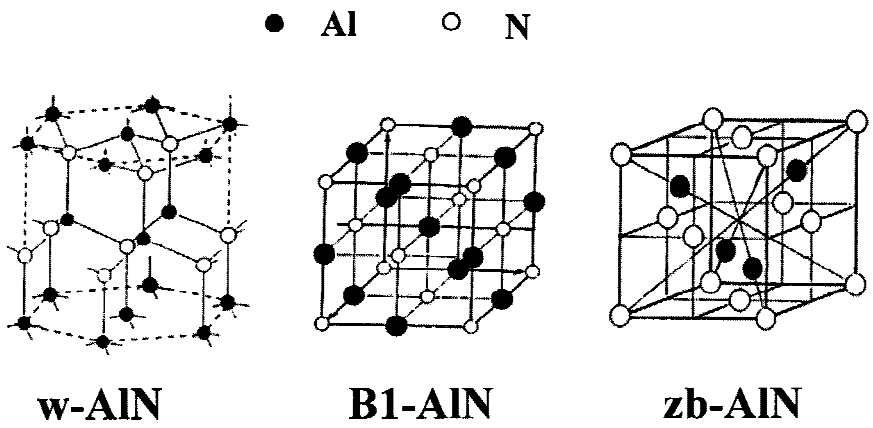

FIG. 1. Schematic of the three structures of AlN.

diffraction (XRD) characterization. A special multilayer sample was grown for the transmission electron microscopy (TEM) study that contained three consecutively grown superlattices with different AlN layer thicknesses, [AlN (1.8 nm)/VN (6.2 nm)]$_3$, [AlN (4.0 nm)/VN (6.2 nm)]$_3$, and [AlN (14.8 nm)/VN (6.2 nm)]$_3$, which enabled observation of both cubic AlN and the w-AlN after the phase transformation in the same sample.

XRD scans were carried out in a double-crystal diffractometer equipped with a LiF focusing monochromator, using the Cu K_α line (0.154 nm). Transmission electron diffraction (TED) and HREM were used to examine the superlattice structures of both the stabilized phase and the transformed phase. Two TEM samples were prepared with different orientations, which enabled high-resolution images to be taken with the electron beam along the MgO [100] and [110] zone axes, respectively. The TEM samples were first mechanically polished to 30 microns and then dimpled to less than 10 microns, after which the samples were ion-milled to electron transparency. The high-resolution images were taken on a Hitachi H-9000 microscope (Hitachi, Tokyo, Japan) operated at 300 kV. Some of the images were high-pass filtered to provide a clearer observation. The filtering removes the electron inelastic scattering effect in the image. The TED patterns were taken on a Hitachi H-8100 microscope using a 20-μm selected area aperture.

III. RESULTS

A. General description of the superlattice layers

Figure 2 shows a low-magnification image of a AlN/VN superlattice with different periodicities with the electron beam along the VN [100] zone axis. The layer thickness of the VN is 6.2 nm. There are two different periods shown in Fig. 2: 10.2 nm with an AlN layer thickness of 4.0 nm and 21.0 nm with an AlN layer thickness of 14.8 nm. The AlN layers appear slightly lighter than the VN layers because of the lower scattering factor of Al. When the AlN layers are thin (4.0-nm layer thickness), a relatively smooth layered structure is present.[8] When the AlN layers grow thicker (14.8-nm layer thickness), the layered structure becomes wavy above the first AlN with 14.8-nm layer thickness.

B. Epitaxial stabilization of B1-AlN in AlN/VN superlattices

Figure 3 shows a higher magnification image of region (a) in Fig. 2, with an inset diffraction pattern. Both the VN and AlN show square lattice fringes. The measured lattice fringe spacing of 2.05 ± 0.03 Å agrees with the theoretical NaCl-type structure lattice parameters (Table I): a_{VN} = 4.14 Å and $a_{B1\text{-}AlN}$ = 4.06 Å, respectively. The diffraction pattern also shows a square symmetry. The diffraction spots are extended along the [002] (growth) direction; this is due to superlattice reflections arising from the artificial periodicity in the structure.[8] The orientation relationship between the two materials is (001)VN//(001)B1-AlN and (010)VN//(010)B1-AlN. No misfit dislocations were observed, which indicates a strained coherent interface between B1-AlN and VN. The same result was observed when the layer thickness of AlN is less than 4.0 nm.

Figure 4 shows a θ–2θ XRD scan of a [AlN (2.7 nm)/VN (2.7 nm)] superlattice. Along with the MgO(002) and the superlattice Bragg peak, small peaks corresponding to the superlattice reflections are present. From the Bragg peak position, the average out-of-plane lattice parameter was 4.10 ± 0.01 Å. This value is between those for VN (4.14 Å) and B1-AlN (4.06 Å).[7] This result is consistent with B1-AlN layers but inconsistent with zb-AlN, which has a significantly larger lattice parameter (4.37 Å). XRD simulations showed a much better fit for B1-AlN than for zb-AlN.[8]

C. Evidence of the AlN phase transformation and residual cubic AlN at the w-AlN/VN interface

Figure 5 shows a higher magnification image of region (b) in Fig. 2. Although the lattice fringes within the VN layer retain a square symmetry, fringes appear in the AlN layer at 4 deg to the AlN/VN interface. The measured *d* spacing in the AlN layer is 2.49 ± 0.03 Å, which matches d_{002} (2.49 Å) of w-AlN,[10] suggesting that a phase transformation has occurred in the thicker AlN material.

A phase transformation from B1-AlN to w-AlN at larger AlN layer thickness was confirmed by XRD. In Fig. 6, a θ–2θ XRD scan of a [AlN (5.0 nm)/VN (2.5 nm)] superlattice, all the superlattice reflections have disappeared. The peak at 36° corresponds to the w-AlN (002) reflection.

Although almost all the AlN has transformed to the wurtzite structure, there does exist a very small fraction of cubic material (<5%). Figure 7 shows a high-resolution image taken at the interface of VN and AlN with an AlN layer thickness exceeding the critical thickness. It was taken with the electron beam along the MgO [100]//VN [100]//B1-AlN [100] direction. Although in the region away from the VN/AlN interface fringes almost parallel to the interface with *d* spacing of 2.49 ± 0.03 Å are found, residuals of square fringes were observed near the film–substrate interface in this particular region. Moiré fringes were also observed in the same region. The square fringes at the VN/AlN interface indicate that there is some residual cubic AlN after the phase transformation. The Moiré fringes suggest the overlapping of multiple structures of B1-AlN and w-AlN. As the (002) planes of w-AlN are at a small angle to the film

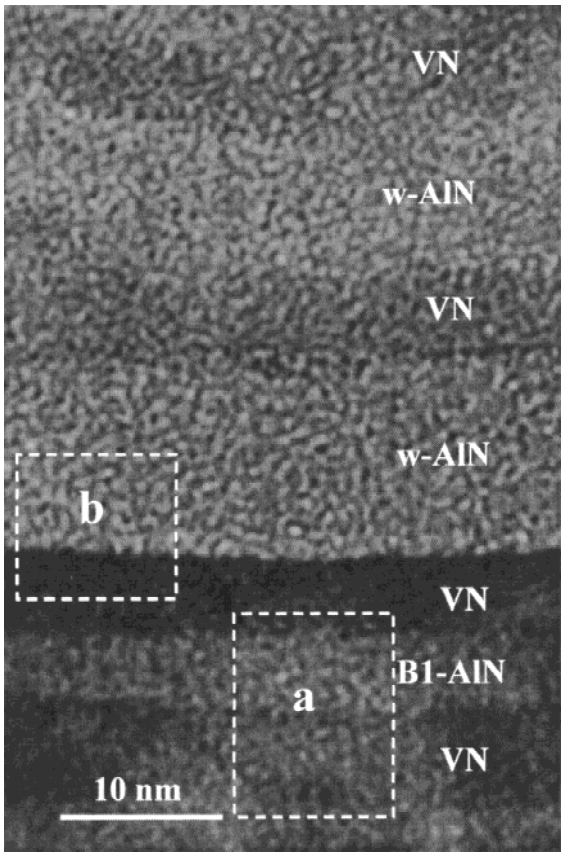

FIG. 2. Image of AlN/VN taken with the electron beam along the MgO [100] direction. A smooth layered structure was observed when the AlN layer thickness is thin. The layered structure became wavy after the B1-wurtzite phase transformation took place.

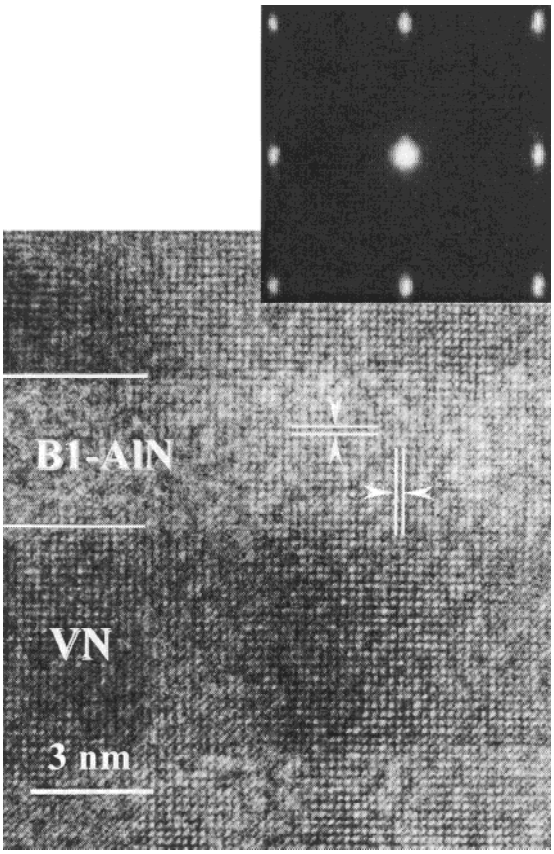

FIG. 3. HREM image of AlN/VN taken several periods away from the MgO substrate with the electron beam along the MgO [100] direction. The layer thickness of AlN was 4.0 nm, and the B1 structure was stabilized in the superlattice. The diffraction pattern in the inset confirmed the cubic structure.

TABLE I. Lattice constants of MgO, VN, zb-AlN, B1-AlN, and w-AlN.

	a (Å)	*c* (Å)
MgO	4.34	…
VN	4.14	…
zb-AlN	4.37	…
B1-AlN	4.06	…
w-AlN	3.11	4.98

interface, a mixed Moiré pattern is formed due to overlapping w-AlN and B1-AlN in a [010] orientation and a small relative twist of the w-AlN (002) planes. The measured *d* spacings from the power spectrum in this region are 2.03 ± 0.04 Å (A), 2.05 ± 0.04 Å (B), and 2.50 ± 0.04 Å (C), which match the *d* spacing of the (002) planes (2.04 Å) of B1-AlN (A, B) and the *d* spacing of the (002) planes (2.49 Å) of w-AlN (C), respectively.

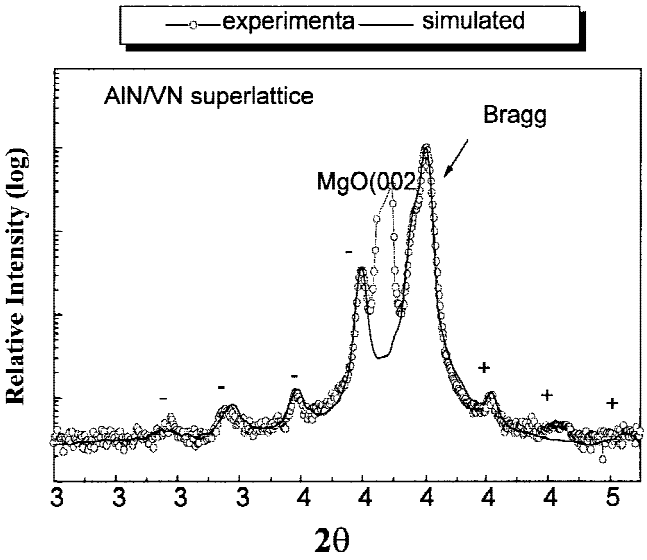

FIG. 4. High-angle XRD of [AlN (1.3 nm)/VN (2.5 nm)] superlattice. The superlattice reflections confirm the B1 structure of AlN.

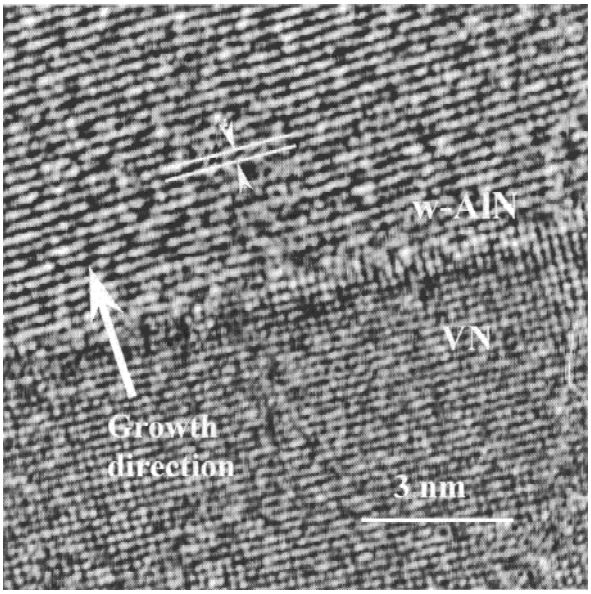

FIG. 5. High-pass filtered HREM image of AlN/VN taken at the interface of w-AlN/VN with the electron beam along the MgO [100] direction. Cubic (002)-type lattice fringes are seen in VN layer, and parallel fringes are seen throughout the w-AlN layer.

D. Orientation of AlN following the phase transformation

Figure 8 shows a selected area diffraction pattern taken from an area which includes the MgO substrate, the B1-AlN/VN (cubic) multilayers, and the w-AlN/VN multilayers. It was taken with the electron beam along

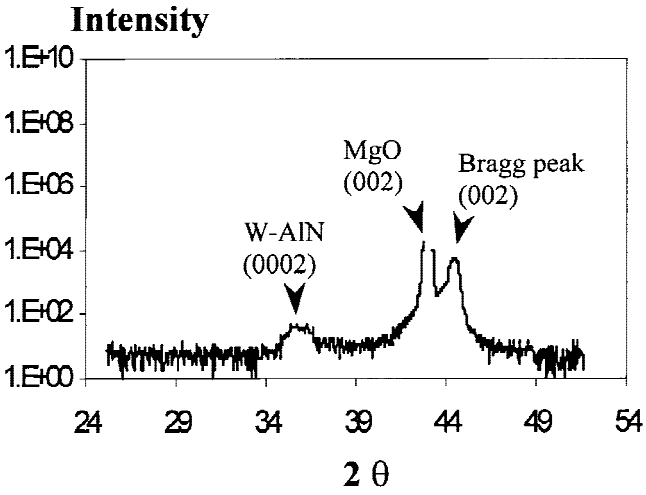

FIG. 6. High-angle XRD of [AlN (5.0 nm)/VN (2.5 nm)] superlattice. No superlattice reflection was observed. The peak at 36 deg corresponds to the w-AlN (002) reflection.

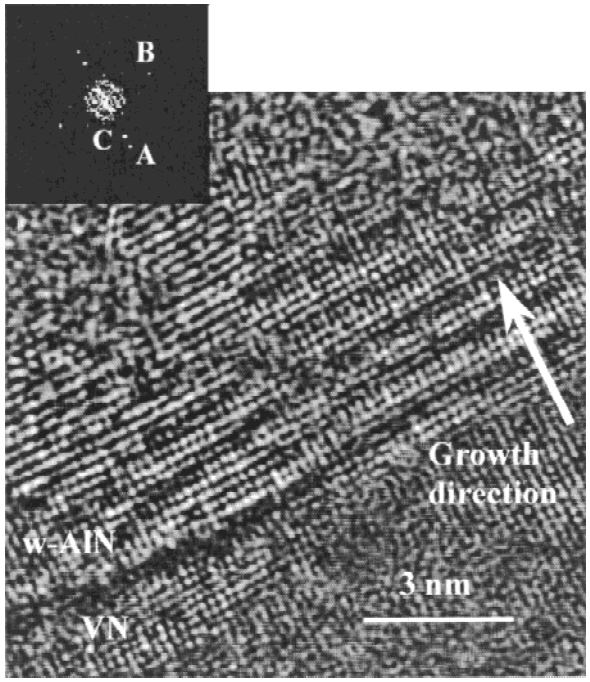

FIG. 7. High-pass filtered HREM image of AlN/VN taken at the interface of w-AlN/VN with the electron beam along the MgO [100] direction. Cubic residuals of AlN are observed at the interface, and Moiré fringes suggest the co-existence of multiple structures. The Power spectrum inset in the upper left was taken from the region of Moiré fringes.

the MgO [110]//[B1-AlN/VN] [110] zone axes. In addition to diffraction spots from the pseudomorphic cubic AlN/VN described above, there are two other sets of spots coming from w-AlN [100] and [120] zone axes, respectively. The orientation relationships are (Fig. 9) the following: I. MgO (002)//[B1-AlN/VN] (002)//w-AlN (002); MgO (110)//[B1-AlN/VN] ($1\bar{1}0$)//w-AlN (010); MgO (110)//[B1-AlN/VN] (110)//w-AlN ($\bar{1}20$). II. MgO (002)//[B1-AlN/VN] (002)//w-AlN (002); MgO ($1\bar{1}0$)//[B1-AlN/VN] ($1\bar{1}0$)//w-AlN ($\bar{1}20$); MgO (110)//[B1-AlN/VN] (110)//w-AlN (010). There are also diffraction spots from a rotated VN layer above the w-AlN layer (not marked here), which will be discussed later.

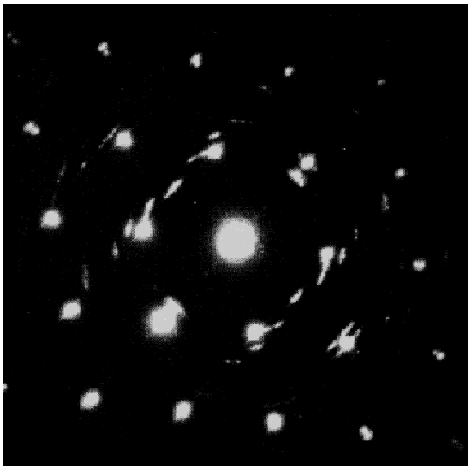

△ Diffraction spots from MgO [110] zone axis

□ Diffraction spots from B1-AlN/VN superlattice [110] zone axis

✤ Diffraction spots from w-AlN [100] zone axis

⬠ Diffraction spots from W-AlN [120] zone axis

FIG. 8. TED pattern taken from the superlattice film. Different symbols are used in the schematic to illustrate the TED pattern.

The images in Figs. 10–12 were taken from different sample regions with the electron beam along the MgO [101] direction. There are three types of fringes in the w-AlN layer: those perpendicular to the AlN/VN interface with a d spacing of 2.70 ± 0.03 Å, which matches a calculated[11] d_{010} (2.69 Å) for w-AlN; those parallel to the interface with a d spacing of 2.49 ± 0.03 Å, which matches d_{002} (2.49 Å) of w-AlN; those at 63/117 deg to the interface with a d spacing of 2.35 ± 0.03 Å, which matches d_{011} (2.37 Å) of w-AlN. These results further confirm the orientations suggested by the diffraction pattern.

E. Orientation of VN after the B1/w-AlN phase transformation

The VN layer deposited after the AlN phase transformation is observed to be reoriented. Figure 13 is taken at the VN/w-AlN interface with the electron beam along the

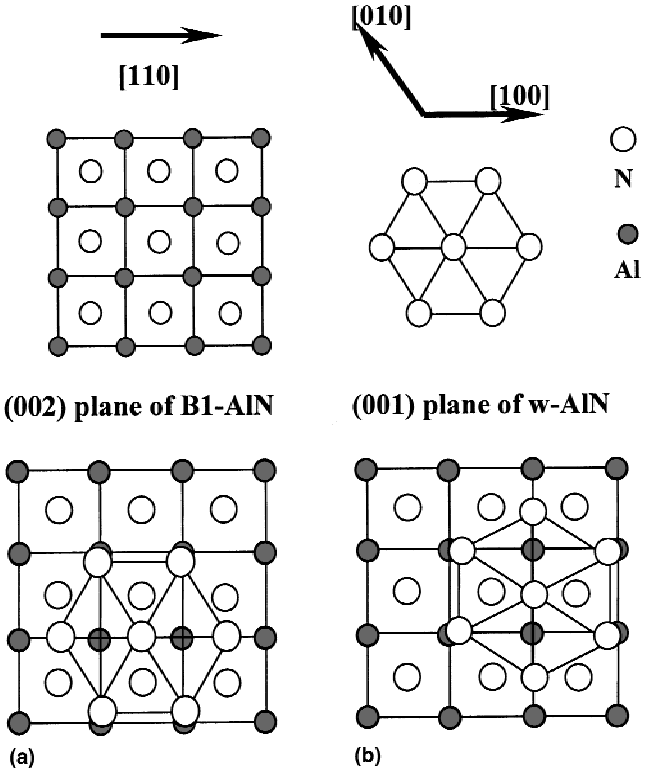

FIG. 9. Two-dimensional model showing one type of epitaxy in w-AlN nucleation on B1-AlN. w-AlN takes the B1-AlN(002) plane as its (002) plane. Its (010) planes match the ($1\bar{1}0$) planes of B1-AlN (a), or its (010) planes match the (110) planes of B1-AlN (b).

MgO [110]//B1-AlN [110]//w-AlN [100] zone axes. It is observed that the VN nucleates by taking the w-AlN (002) plane as its (111) plane instead of the (002) plane. This is also supported by the diffraction pattern in the inset of Fig. 13.

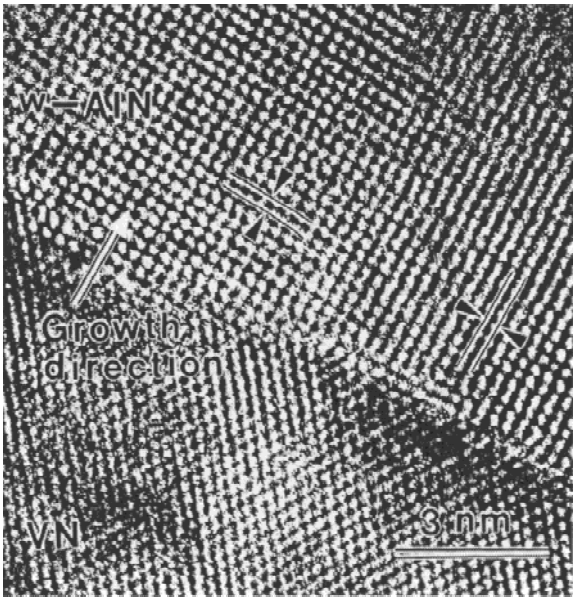

FIG. 10. HREM image of AlN/VN superlattice taken at the interface of the first transformed layer of w-AlN and VN with the electron beam along the MgO [110] direction. There are two types of the fringes in the w-AlN layer—those perpendicular to the w-AlN/VN interface and those parallel to the interface.

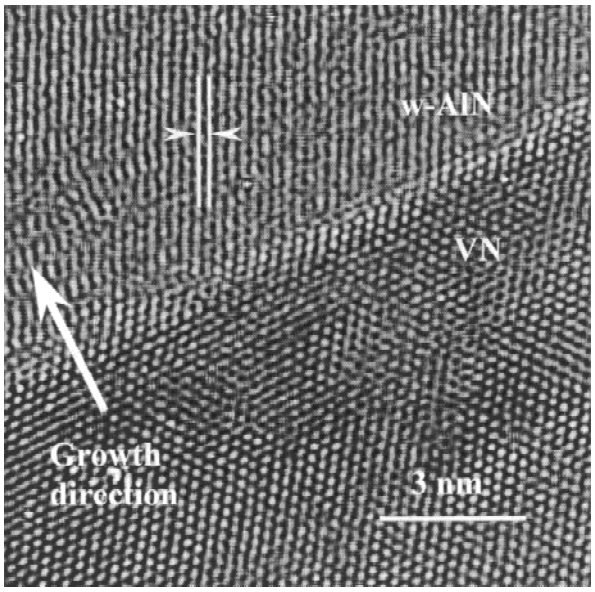

FIG. 11. High-pass filtered HREM image of an AlN/VN superlattice taken at the interface of the first transformed layer of w-AlN and VN with the electron beam along the MgO [110] direction. There is another type of fringe shown in the w-AlN layer at 63 deg to the interface.

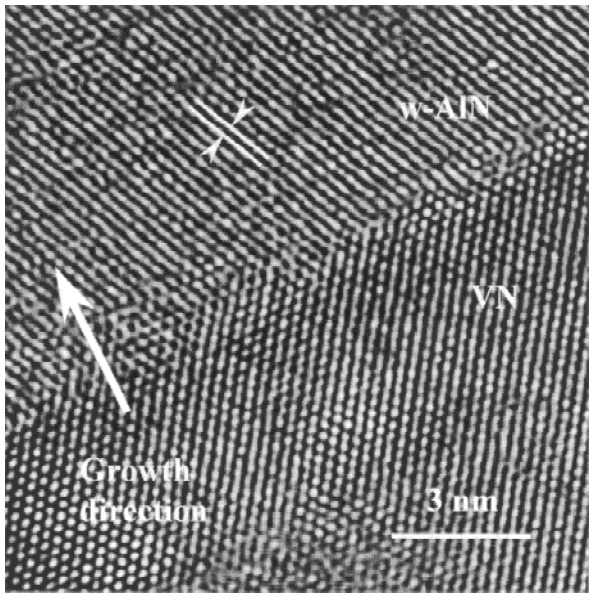

FIG. 12. Fringes shown in the w-AlN layer are the same type as those shown in Fig. 9, but at 117 deg to the w-AlN/VN interface.

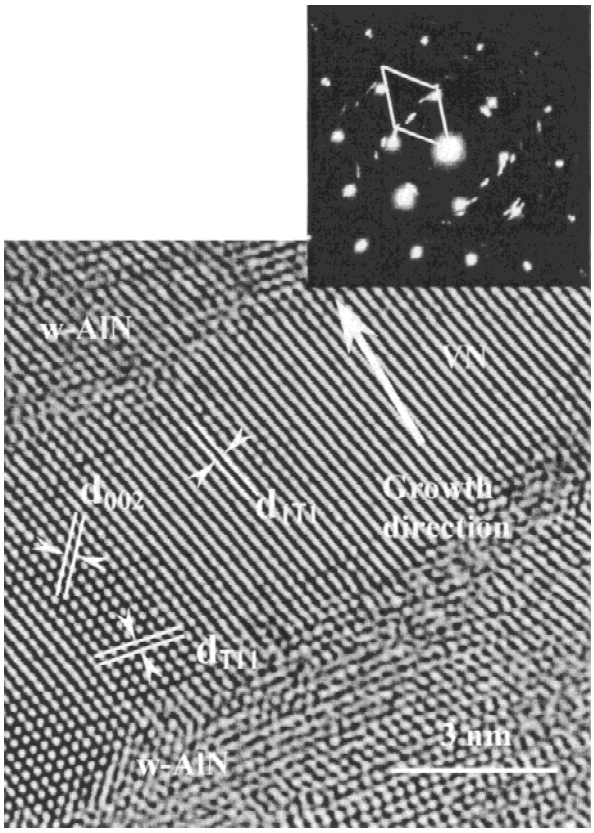

FIG. 13. High-pass filtered HREM images of w-AlN/VN/w-AlN taken with the electron beam along the MgO [110] direction. The (002) plane of VN was reorientated to its (111) plane position in the B1-AlN/VN multilayer. The diffraction pattern in the inset showed the diffraction spot from reorientated VN [110] zone axis.

IV. DISCUSSION

The experimental evidence demonstrates that metastable B1-AlN is stabilized in AlN/VN superlattices when the AlN layers are sufficiently thin. The stabilization of B1-AlN can be explained using a simple energy argument.[7] The total energy per formula unit area of an AlN layer during growth can be written as

$$E_{\text{Total}} = (E_{\text{B}} + E_{\text{S}})l + E_{\text{I}} \quad ,$$

where E_{B} is the strain-free bulk energy, E_{S} the coherency strain energy, E_{I} the interfacial energy, and l the thickness of the growing AlN layer. Although the strain free bulk energy of B1-AlN is larger than that of wurzite AlN, it is possible for AlN to grow with the B1-structure if it forms a coherent interface with the underlying material (smaller E_{S} and E_{I}), while the lower bulk energy wurzite AlN does not. The metastable B1-AlN would grow at small layer thickness when the interfacial energy dominates the bulk energy but transform to the wurzite phase when the bulk energy becomes dominant. A phase transformation from B1 to w-AlN takes place when the thickness of AlN exceeds a critical thickness of approximately 3.0–4.0 nm, depending on the VN layer thickness.[8] In this thicker AlN layer growth, AlN grows in the B1 structure initially and then transforms to hexagonal with the initially B1 layer transforming. Once this phase transition occurs, further growth of VN onto the w-AlN is still epitaxial but with a different orientation relative to the substrate VN. Because the w-AlN has two possible orientations with a slight tilt, in an XRD measurement it might appear that the VN is completely misoriented and all epitaxial information lost, but this is not the case.

The particular orientations of the w-AlN on the initially-grown B1-AlN, as well as the subsequent growth of VN on the transformed w-AlN, can be understood via simple interface symmetry and lattice matching arguments. There are two plausible orientations for the transformed w-AlN, the one we observed (see Fig. 9) or one with a common close-packed N plane [i.e., (111) in the B1 and the basal plane in the w-AlN], as shown in Fig. 14. [The latter would correspond to a dislocation driven phase transformation normally observed in fcc-hcp phase transition,[12] which takes place by the passage of a partial dislocation $a/6\langle 112\rangle$ on the {111} FCC planes, with the (111) planes of the cubic structure the basal planes of the HCP structure.] Taking the observed lattice parameter of the AlN/VN cubic multilayer (4.10 Å), the observed orientation has a smaller misfit of 6.8% (along the w-AlN [120]//B1-AlN [$\bar{1}$10] direction) compared to 7.9% (along the w-AlN [120]//B1-AlN [$\bar{1}$12] direction) in the other orientation (Table II); the N–N distances are smaller in B1-AlN[7] than they are in w-AlN. There are two equivalent orientations for this epitaxy, at 90° to each other (Fig. 9). There is a tilt of about 4° that probably helps to accommodate the misfit. The same orientation is not observed for the later growth of relaxed VN on the w-AlN because VN has a 1% larger lattice parameter (4.14 Å). Therefore the other orientation (common close-packed cation planes) has a smaller

TABLE II. Comparison of the in-plane lattice mismatch of B1-AlN/w-AlN and w-AlN/VN interfaces.

		Lattice constant along different directions (Å)	
		x	*y*
1	Strained B1-AlN (002)	[110] 2.88	2 [$\bar{1}$10] 5.77
2	Strained B1-AlN (111)	[110] 2.88	[$\bar{1}$12] 4.98
3	w-AlN (001)	[100] 3.11	[120] 5.39
4	VN (002)	[110] 2.93	2 [$\bar{1}$10] 5.86
5	VN (111)	[110] 2.93	[$\bar{1}$12] 5.07

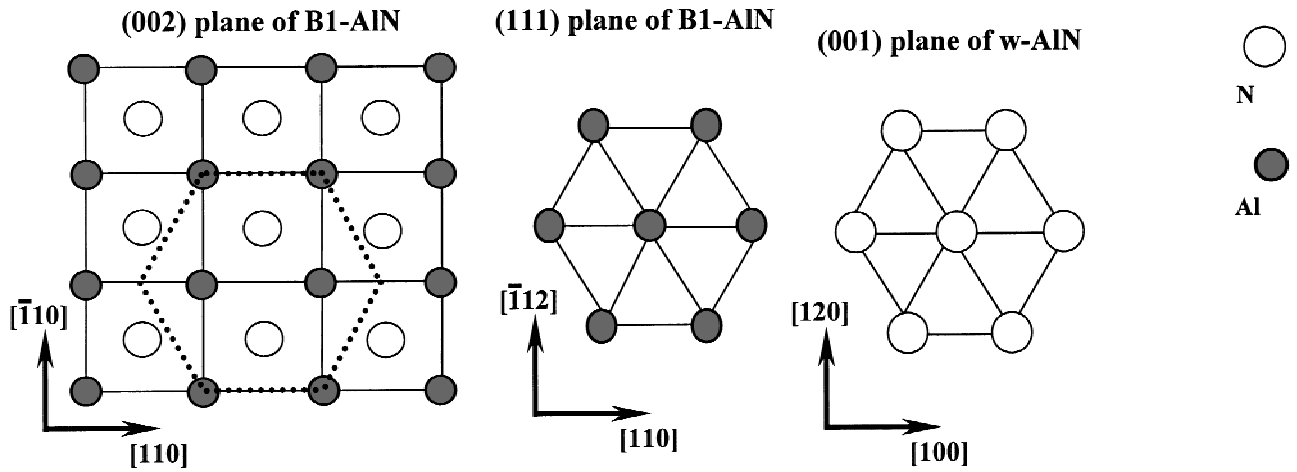

FIG. 14. Comparison of the B1-AlN (VN) (002) plane, (111) plane, and w-AlN (002) plane.

misfit of 6.1% (along the VN [$\bar{1}$12]//w-AlN [120] direction) compared to that of 8.2% (along the VN [$\bar{1}$10]//w-AlN [120] direction); this orientation will also be favored by a hexagonal–hexagonal symmetry match. Unfortunately the experimental interfaces after the transformation are too rough for precise HREM to determine the atomistic interface structure or make statements about the possible presence of interface dislocations.

While it is not possible to state in atomistic detail exactly what takes place during the phase transition from B1-AlN to w-AlN, the presence of retained untransformed B1-AlN left at the AlN/VN interface (Fig. 7) suggests that the phase transformation started at the free surface of AlN during deposition.

V. CONCLUSIONS

In conclusion, B1-AlN was epitaxially stabilized in AlN/VN superlattices when the AlN layer thickness is less than 4 nm. B1-AlN transformed to w-AlN at larger AlN layer thicknesses. There were two domains of the transformed w-AlN, i.e., the following: I. [B1-AlN/VN] (002)//w-AlN (002); [B1-AlN/VN] (110)//w-AlN (010); [B1-AlN/VN] (110)//w-AlN ($\bar{1}$20). II. [B1-AlN/VN] (002)//w-AlN (002); [B1-AlN/VN] ($\bar{1}$10)//w-AlN($\bar{1}$20); [B1-AlN/VN] (110)//w-AlN(010).

The VN layer deposited after the B1/w-AlN phase transformation was reoriented compared to the VN in the B1-AlN/VN superlattice. The orientations of the w-AlN on the (strained) B1-AlN and the subsequent growth of (relaxed) VN on the transformed w-AlN were explained by the crystal symmetry and minimization of lattice misfit. The very small fraction of retained B1-AlN at the interface of VN and w-AlN suggested that the phase transformation started at the free surface of B1-AlN during deposition.

ACKNOWLEDGMENT

This work was supported by the MRSEC program of the National Science Foundation (DMR-9632472) at the Materials Research Center of Northwestern University.

REFERENCES

1. N.E. Christensen and I. Gorczyca, Phys. Rev. B **50,** 4397 (1994).
2. W. Kohn and L.J. Sham, Phys. Rev. A.**140,** 1133 (1965).
3. M. Ueno, A. Onodera, O. Shimomura, and K. Takemura, Phys. Rev. B **45,** 10123 (1992).
4. Q. Xia, H. Xia, and A.L. Ruoff, J. Appl. Phys. **73,** 8198 (1993).
5. I.W. Kim, A. Madan, M.W. Guruz, V.P. Dravid, and S.A. Barnett, J. Vac. Sci. Technol., A **19,** 2069 (2001).
6. A. Madan, I.W. Kim, and S.A. Barnett (unpublished, 1996).
7. A. Madan, I.W. Kim, S.C. Cheng, P. Yashar, V.P. Dravid, and S.A. Barnett, Phys. Rev. Lett. **78,** 1743 (1997).
8. I.W. Kim, Q. Li, L.D. Marks, and S.A. Barnett, Appl. Phys. Lett. **78,** 892 (2001).
9. P.B. Mirkarimi, M. Shinn, and S.A. Barnett, J. Vac. Sci. Technol., A **10,** 1618 (1992).
10. H. Schulz and K. Thiemann, Solid State Commun. **23,** 815 (1977).
11. J.W. Edington, *Monographs in Practical Electron Microscopy in Material Science, II, Electron Diffraction in the Electron Microscope* (Macmillan, London, 1975).
12. A.K. Jena and M.C. Chaturvedi, *Phase Transformations in Materials* (Prentice Hall, Englewood Cliffs, NJ, 1992).